

The dynamics of starvation and recovery

² Justin D. Yeakel * †‡, Christopher P. Kempes †, and Sidney Redner †§

³ *School of Natural Science, University of California Merced, Merced, CA, †The Santa Fe Institute, Santa Fe, NM, §Department of Physics, Boston University, Boston
⁴ MA, and ‡To whom correspondence should be addressed: jdyeakel@gmail.com

⁵ Submitted to Proceedings of the National Academy of Sciences of the United States of America

This is the abstract. [No it isn't. It's merely a placeholder.]

foraging | starvation | reproduction

Introduction

The behavioral ecology of most, if not all, organisms is influenced by the energetic state of individuals, which directly influences how they invest reserves in uncertain environments. Such behaviors are generally manifested as trade-offs between investing in somatic maintenance and growth, or allocating energy towards reproduction [1, 2, 3]. The timing of these behaviors responds to selective pressure, as the choice of the investment impacts future fitness [4]. The influence of resource limitation on an organism's ability to maintain its nutritional stores may lead to repeated delays or shifts in reproduction over the course of an organism's life.

The life history of most species is typically comprised of (a) somatic growth and maintenance, and (b) reproduction. The balance between these two activities is often conditioned on resource availability [5]. For example, reindeer invest less in calves born after harsh winters (when the mother's energetic state is depleted) than in calves born after moderate winters [6]. Many bird species invest differently in broods during periods of resource scarcity compared to normal periods [7, 8], sometimes delaying or even foregoing reproduction for a breeding season [1, 9, 10]. Even freshwater and marine zooplankton have been observed to avoid reproduction under nutritional stress [11], and those that do reproduce have lower survival rates [2]. Organisms may also separate maintenance and growth from reproduction over space and time: many salmonids, birds, and some mammals return to migratory breeding grounds to reproduce after one or multiple seasons in resource-rich environments where they accumulate nutritional reserves [12, 13, 14].

Physiological mechanisms also play an important role in regulating reproductive expenditures during periods of resource limitation. The data collected thus far has shown that diverse mammals (47 species in 10 families) exhibit delayed implantation, whereby females postpone fetal development (blastocyst implantation) until times where nutritional reserves can be accumulated [15, 16]. Many other many species (including humans) suffer irregular menstrual cycling and higher spontaneous abortion rates during periods of nutritional stress [17, 18]. In the extreme case of unicellular organisms, nutrition is unavoidably linked to reproduction because the nutritional state of the cell regulates all aspects of the cell cycle [19]. The existence of so many independently evolved mechanisms across such a diverse suite of organisms highlights the importance and universality of the fundamental tradeoff between somatic and reproductive investment. However the dynamic implications of these constraints are unknown.

Though straightforward conceptually, incorporating the energetic dynamics of individuals [20] into a population-level framework [20, 21] presents numerous mathematical obstacles [22]. An alternative approach involves modeling the macroscale relations that guide somatic versus reproductive investment in a consumer-resource system. For example, macroscale Lotka-Volterra models assume that the growth rate of the consumer population depends on resource density, thus

implicitly incorporating the requirement of resource availability for reproduction [23].

In this work, we adopt an alternative approach in which resource limitation and the subsequent effect of starvation is accounted for explicitly. Namely, only individuals with sufficient energetic reserves can reproduce. Such a constraint leads to reproductive time lags due to some members of the population going hungry and then recovering. Additionally, we incorporate the idea that reproduction is strongly constrained allometrically [3], and is not generally linearly related to resource density. As we shall show, these constraints influence the ensuing population dynamics in dramatic ways.

Nutritional-state-structured model (NSM)

We begin by defining a minimal Nutritional-State-structured population Model (NSM), where the consumer population is divided into two energetic states: (a) an energetically replete (full) state F , where the consumer reproduces at a constant rate λ and has no mortality risk, and (b) an energetically deficient (hungry) state H , where the consumer does not reproduce but dies at rate μ . The underlying resource R evolves by logistic growth with an intrinsic growth rate α and a carrying capacity equal to one. Consumers transition from the full state F to the hungry state H at a rate σ —the starvation rate—and also in proportion to the absence of resources $(1 - R)$. Conversely, consumers recover from state H to state F at rate ρ and in proportion to R . Resources are also eaten by the consumers—at rate ρ by hungry consumers and at rate $\beta < \rho$ by full consumers. This inequality accounts for hungry consumers requiring more resources to rebuild body weight.

In the mean-field approximation, in which the consumers and resources are perfectly mixed, their densities evolve according to the rate equations

$$\begin{aligned}\dot{F} &= \lambda F + \rho RH - \sigma(1 - R)F, \\ \dot{H} &= \sigma(1 - R)F - \rho RH - \mu H, \\ \dot{R} &= \alpha R(1 - R) - R(\rho H + \beta F).\end{aligned}\quad [1]$$

Notice that the total consumer density $F + H$ evolves according to $\dot{F} + \dot{H} = \lambda F - \mu H$. This resembles the equation of motion for the predator density in the classic Lotka-Volterra model, except that the resource density does not appear in the growth term. As discussed above, the attributes of reproduction and mortality have been explicitly apportioned to the full and hungry consumers, respectively, so that the growth in the total density is decoupled from the resource density.

Reserved for Publication Footnotes

103 Equation [1] has three fixed points: two trivial fixed points 161 If ρ exceeds a threshold value, cyclic dynamics will develop as
 104 at $(F^*, H^*, R^*) = (0, 0, 0)$ and $(0, 0, 1)$, and one non-trivial, 162 the Hopf bifurcation is approached.
 105 internal fixed point at

$$F^* = \frac{\alpha\lambda\mu(\mu + \rho)}{(\lambda\rho + \mu\sigma)(\lambda\rho + \mu\beta)},$$

$$H^* = \frac{\alpha\lambda^2(\mu + \rho)}{(\lambda\rho + \mu\sigma)(\lambda\rho + \mu\beta)},$$

$$R^* = \frac{\mu(\sigma - \lambda)}{\lambda\rho + \mu\sigma}.$$

106 The stability of this fixed point is determined by the Jaco- 161
 107 bian Matrix \mathbf{J} , where each matrix element J_{ij} equals $\partial\dot{X}_i/\partial X_j$
 108 when evaluated at the internal fixed point, and \mathbf{X} is the vec- 162
 109 tor (F, H, R) . The parameters in Eq. [1] are such that the 163
 110 real part of the largest eigenvalue of \mathbf{J} is negative, so that the 164
 111 system is stable with respect to small perturbations from the 165
 112 fixed point. Because this fixed point is unique, it is the global 166
 113 attractor for all population trajectories for any initial condition 167
 114 where the resource and consumer densities are both non zero. 168

115 From Eq. [2], an obvious constraint on the NSM is that 169
 116 the reproduction rate λ must be less than the starvation rate 170
 117 σ , so that R^* is positive. In fact, when the resource density 171
 118 $R = 0$, the rate equation for F gives exponential growth of 172
 119 F for $\lambda > \sigma$. The condition $\sigma = \lambda$ represents a transcritical 173
 120 (TC) bifurcation that demarcates the physical and unphysical 174
 121 regimes [give Ref]. The biological implication of the constraint 175
 122 $\lambda < \sigma$ has a simple interpretation—the rate at which a macro- 176
 123 scopic organism loses mass due to lack of resources is generally 177
 124 much faster than the rate of reproduction. As we will discuss 178
 125 below, this inequality is a natural consequence of allometric 179
 126 constraints [3] for organisms within empirically observed body 180
 127 size ranges (Fig. 2).

128 In the physical regime of $\lambda < \sigma$, the fixed point [2] may 181
 129 either be a stable node or a limit cycle (Fig. 3). In continuous- 182
 130 time systems, a limit cycle arises when a pair of complex con- 183
 131 jugate eigenvalues crosses the imaginary axis to attain positive 184
 132 real parts [24]. This Hopf bifurcation is defined by $\text{Det}(\mathbf{S}) = 0$, 185
 133 with \mathbf{S} the Sylvester matrix, which is composed of the coef- 186
 134 ficients of the characteristic polynomial of the Jacobian ma- 187
 135 trix [25]. As the system parameters are tuned to be within the 188
 136 stable regime but close to the Hopf bifurcation, the amplitude of 189
 137 the transient but decaying cycles become large. Given that eco- 190
 138 logical systems are constantly being perturbed [26], the onset of 191
 139 transient cycles, even though they decay with time in the mean- 192
 140 field description, can increase the extinction risk [27, 28, 29]. 193
 141 Thus the distance of a system from the Hopf bifurcation pro- 194
 142 vides a measure of its persistence.

143 When the starvation rate $\sigma \gg \lambda$, a substantial fraction 195
 144 of the consumers are driven to the hungry non-reproducing 196
 145 state. Because reproduction is inhibited, there is a low steady- 197
 146 state consumer density and a high steady-state resource den- 198
 147 sity. However, if $\sigma/\lambda \rightarrow 1$ from above, the population is 199
 148 overloaded with energetically-replete (reproducing) individuals, 200
 149 thereby promoting oscillations between the consumer and re- 201
 150 source densities (Fig. 3).

151 Whereas the relation between consumer growth rate λ and 202
 152 the starvation rate σ defines an absolute bound of biological 203
 153 feasibility—the TC bifurcation—the starvation rate σ also de- 204
 154 termines the sensitivity of the consumer population to changes 205
 155 in resource density. When $\sigma \gg \lambda$, the steady-state population 206
 156 density is small, thereby increasing the risk of stochastic ex- 207
 157 tinction. On the other hand, as σ decreases, the system will 208
 158 ultimately be poised either near the TC or the Hopf bifurcation 209
 159 (Fig. 3). If the recovery rate ρ is sufficiently small, the TC bi- 210
 160 furcation is reached and the resource eventually is eliminated.

163 [mention and refer to the starving random walk
 164 model somewhere.]

165 Role of allometry

166 The NSM describes a broad range of dynamics, yet organisms 167
 168 are likely unable to access most of the total parameter space. 169
 170 Here we use allometric scaling relations to constrain the covaria- 171
 172 tion of rates in a principled and biologically meaningful manner. 173
 173 Allometric scaling relations highlight common constraints and 174
 174 average trends across large ranges in body size and species di- 175
 175 versity. Many of these relations can be derived from a small set 176
 176 of assumptions and below we describe a framework to deter- 177
 177 mine the covariation of timescales and rates across the range of 178
 178 mammals for each of the key parameters of our model (cf. [30]). 179
 179 We are thereby able to define the regime of dynamics occupied 180
 180 by the entire class of mammals along with the key differences 181
 181 between the largest and smallest mammals.

182 Nearly all of the rates described in the NSM are to some 183 extent governed by consumer metabolism, which can be used 184 to describe a variety of organismal features [31]. The scaling 185 relation between an organism's metabolic rate B and its body 186 size at reproductive maturity M is well documented [32] and 187 scales as $B = B_0 M^\eta$, where η is the scaling exponent, gen- 188 erally assumed to vary around 2/3 or 3/4 for metazoans (e.g. 189 [31]), and has taxonomic shifts for unicellular species between 190 $\eta \approx 1$ in eukaryotes and $\eta \approx 1.76$ in bacteria [33, 3]. Several 191 efforts have shown how a partitioning of this metabolic rate be- 192 tween growth and maintenance purposes can be used to derive a 193 general equation for the growth trajectories and growth rates of 194 organisms ranging from bacteria to metazoans [34, 35, 36, 37, 3]. 195 More specifically, the cross-species trends in growth rate can be 196 approximated by

$$\lambda = \lambda_0 M^{\eta-1}. \quad [3]$$

197 This relation is derived from the simple balance condition 198 [34, 35, 36, 37, 3]

$$B_0 m^\eta = E_m \frac{dm}{dt} + B_m m, \quad [4]$$

199 where E_m is the energy needed to synthesize a unit of mass, 200 B_m is the metabolic rate to support an existing unit of mass, 201 and m is the mass at any point in development. This balance 202 has the general solution [35, 3]

$$m(t) = \left[1 - \left(1 - \frac{b}{a} m_0^{1-\eta} \right) e^{-b(1-\eta)t} \right]^{1/(1-\eta)} \left(\frac{a}{b} \right)^{1/(1-\eta)} \quad [5]$$

203 where, $a = B_0/E_m$ and $b = B_m/E_m$, and which we use to 204 define the timescale of recovery from starvation. The rate of 205 recovery $\rho = 1/t_\rho$ requires that an organism accrues sufficient 206 tissue to transition from the hungry to the full state. Since 207 only certain tissues can be digested for energy (for example the 208 brain cannot be degraded to fuel metabolism), we define the rate 209 for starvation, death, and recovery by the timescales required 210 to reach, or return from, specific fractions of the replete-state 211 mass. We define $m_{\text{starve}} = \epsilon M$, where $\epsilon < 1$ is the fraction 212 of replete-state mass where reproduction ceases. This fraction 213 will be modified if tissue composition systematically scales with 214 adult mass. For example, making use of the observation that 215 body fat in mammals scales with overall body size according to 216 $M_f = f_0 M^\gamma$ and assuming that once this mass is fully digested 217 the organism starves, this would imply that $\epsilon = 1 - f_0 M^\gamma/M$. 218 It follows that the recovery timescale, $t_\rho = t_2 - t_1$, is the time 219 it takes to go from $m(t_1) = \epsilon M$ to $m(t_2) = M$, or

$$t_\rho = \frac{\ln \left[1 - \frac{a}{b} (M)^{1-\eta} \right] - \ln \left[1 - \frac{a}{b} (\epsilon M)^{1-\eta} \right]}{(\eta - 1)b}. \quad [6]$$

218 It should be noted that more complicated ontogenetic models 274 to population oscillations—including both stable limit cycles as
 219 explicitly handle storage [37], whereas this is implicitly covered 275 well as transient cycles—than mammals with larger body size.
 220 by the body fat scaling in our framework.

221 To determine the starvation rate, σ , we are interested in 277 less common for larger species and more common for smaller
 222 the time required for an organism to go from a mature adult 278 species, particularly in environments where resources are limit-
 223 that reproduces at rate λ (henceforth we term this state as the 279 ing.

224 “replete” state), to a reduced-mass hungry state where repro- 280 Previous studies have used allometric constraints to explain
 225 duction is impossible. For starving individuals we assume that 281 the periodicity of cyclic populations [39, 40, 41], suggesting a pe-
 226 an organism must meet its maintenance requirements using the 282 riod $\propto M^{0.25}$, however this relation seems to hold only for some
 227 digestion of existing mass as the sole energy source. This as- 283 species [42] and competing explanations [related to[??]] ex-
 228 sumption implies the following simple metabolic balance 284 ist [43, 44]. Statistically significant support for the existence of
 229 trajectory of a non-consuming organism:

$$\frac{dm}{dt} E'_m = -B_m m$$

229 where E'_m is the amount of energy stored in a unit of exist-
 230 ing body mass which differs from E_m , the energy required to
 231 synthesize a unit of biomass [37]. Given the replete mass, M ,
 232 of an organism, the above energy balance prescribes the mass
 233 trajectory of a non-consuming organism:

$$m(t) = M e^{-b't}$$

234 where $b' = E'_m / B_m$. The time scale for starvation is given
 235 by the time it takes this decay to reach ϵM , which is

$$t_\sigma = -b' \ln(\epsilon).$$

236 The starvation rate is then $\sigma = 1/t_\sigma$, which scales with replete-
 237 state mass as $1/\ln(1 - f_0 M^\gamma / M)$. An important feature is
 238 that σ does not have a simple scaling dependence on λ (Eq. 3),
 239 which is important for the dynamics that we later discuss.

240 The time to death should follow a similar relation, but de-
 241 fined by a lower fraction of replete-state mass, $m_{\text{death}} = \epsilon' M$.
 242 Suppose, for example, that an organism dies once it has di-
 243 gested all fat and muscle tissues, and that muscle tissue scales
 244 with body mass according to $M_m = u_0 M^\zeta$. This gives $\epsilon' =$
 245 $1 - (f_0 M^\gamma + u_0 M^\zeta) / M$. Muscle mass has been shown to be
 246 roughly proportional to body mass [38] in mammals and thus
 247 ϵ' is merely ϵ minus a constant. Thus

$$t_\mu = -b' \ln(\epsilon')$$

248 and $\mu = 1/t_\mu$.

249 Although these rate equations are general, here we focus on
 250 parameterizations for terrestrial-bound endotherms, specifically
 251 mammals, which range from a minimum of $M \approx 1$ gram (the
 252 Etruscan shrew *Suncus etruscus*) to a maximum of $M \approx 10^7$
 253 grams (the late Eocene to early Miocene Indricotheriinae). In-
 254 vestigating other classes of organisms would simply involve al-
 255 tering the metabolic exponents and scalings associate with ϵ .
 256 Moreover, we emphasize that our allometric equations describe
 257 mean relationships, and do not account for the (sometimes con-
 258 siderable) variance associated with individual species.

260 Stabilizing effects of allometric constraints

261 As the allometric derivations of the NSM rate laws reveal, σ and
 262 ρ are not independent parameters, and the bifurcation space
 263 shown in Fig. 3 is navigated via covarying parameters. Given
 264 the parameters of terrestrial endotherms, we find that σ and ρ
 265 are constrained to lie within a small window of potential values
 266 (Fig. 4) for the known range of body sizes M . We thus find that
 267 the dynamics for all mammalian body sizes is confined to the
 268 steady-state regime of the NSM and that limit-cycle behavior
 269 is precluded. Moreover, for larger M , the distance to the Hopf
 270 bifurcation increases, while uncertainty in allometric param-
 271 ters (20% variation around the mean; Fig. 4) results in little
 272 qualitative difference in the distance to the the Hopf bifurca-
 273 tion. These results suggest that small mammals are more prone

276 Thus our NSM model predicts that population cycles should be
 277 well as transient cycles—than mammals with larger body size.
 278 species [42] and competing explanations [related to[??]] ex-
 279 ist [43, 44]. Statistically significant support for the existence of
 280 Previous studies have used allometric constraints to explain
 281 the periodicity of cyclic populations [39, 40, 41], suggesting a pe-
 282 riod $\propto M^{0.25}$, however this relation seems to hold only for some
 283 species [42] and competing explanations [related to[??]] ex-
 284 ist [43, 44]. Statistically significant support for the existence of
 285 population cycles among mammals is predominantly based on
 286 time series for small mammals [45], where we our model would
 287 predict much longer and more pronounced transient dynamics,
 288 given how close these points are to the Hopf bifurcation. On
 289 the other hand, the longer gestational times and the increased
 290 difficulty in measurements, precludes obtaining similar-quality
 291 data for larger organisms.

292 Extinction risk

293 Within our model, higher rates of starvation result in a larger
 294 flux of the population to the hungry state. In this state repro-
 295 duction is absent, thus increasing the likelihood of extinction.
 296 However, from the perspective of population survival, it is the
 297 rate of starvation relative to the rate of recovery that deter-
 298 mines the long-term dynamics of the system (Fig. 3). We now
 299 examine the competing effects of cyclic dynamics vs. changes in
 300 steady state density on extinction risk as a function of the ratio
 301 σ/ρ . To this end, we computed the probability of extinction,
 302 where extinction is defined as the population trajectory going
 303 below $0.2 \times$ the allometrically constrained steady state for all
 304 times between 10^2 and $\leq 10^6$. This procedure is repeated for
 305 1000 replicates of the continuous-time system shown in Eq. 1
 306 for an organism of $M = 100$ grams. In each replicate the initial
 307 condition is distributed around the steady state (Eq. 2). Specif-
 308 ically the initial densities are chosen to be $A(F^*, H^*, R^*)$, with
 309 A a random variable that is uniformly distribution in $[0, 2]$. By
 310 allowing the rate of starvation to vary, we assessed extinction
 311 risk across a range of values of the ratio σ/ρ varying between
 312 10^{-2} to 2.5 , thus examining a horizontal cross-section of Fig. 3.

313 As expected, higher rates of extinction correlated with both low
 314 and high values of σ/ρ . For low values of σ/ρ , the increased
 315 extinction risk results from transient cycles with larger ampli-
 316 tudes as the system nears the Hopf bifurcation (Fig. 5). For
 317 large values of σ/ρ , higher extinction risk arises because of to
 318 the decrease in the steady state consumer population density.
 319 This interplay creates an ‘extinction refuge’ as shown in Fig. 5,
 320 such that for a relatively constrained range of σ/ρ , extinction
 321 probabilities are minimized.

322 We find that the allometrically constrained values of σ/ρ
 323 (with $\pm 20\%$ variability around energetic parameter means) fall
 324 within the extinction refuge. These values are close enough to
 325 the Hopf bifurcation to avoid low steady state densities, and
 326 far enough away to avoid large-amplitude transient cycles. The
 327 fact that allometric values of σ and ρ fall within this relatively
 328 small window supports the possibility that a selective mech-
 329 nism has constrained the physiological conditions that drive ob-
 330 served starvation and recovery rates within populations. Such a
 331 mechanism would select for organism physiology that generates
 332 appropriate σ and ρ values that avoid extinction. This selection
 333 could occur via the tuning of body fat percentages, metabolic
 334 rates, and biomass maintenance efficiencies. To summarize,
 335 our finding that the allometrically-determined parameters fall
 336 within this low extinction probability region suggests that the
 337 NSM dynamics may both drive—and constrain—natural ani-
 338 mal populations.

341 **Dynamic and energetic barriers to body size**

342 Metabolite transport constraints are widely thought to place 393 noted by ') where individuals have a modified proportion of
 343 strict boundaries on biological scaling [46, 47, 31] and thereby 394 body fat $M' = M(1 + \chi)$ where $\chi \in [-0.5, 0.5]$, thus al-
 344 lead to specific predictions on the minimum possible body size 395 tering the rates of starvation σ , recovery ρ , and maintenance
 345 for organisms [48]. Above this bound, a number of energetic and 396 β . There is no internal fixed point that correspond to a state
 346 evolutionary mechanisms have been explored to assess the costs 397 where both original residents and invaders coexist (except for
 347 and benefits associated with larger body masses, particularly 398 the trivial state $\chi = 0$). To assess the susceptibility to in-
 348 for mammals. One important such example is the *fasting en-* 399 vasion as a function of the invader mass, we determine which
 349 *durance hypothesis*, which contends that larger body size, with 400 consumer has a higher steady-state density for a given value of
 350 consequent lower metabolic rates and increased ability to main- 401 χ . We find that for $1 \leq M < 10^6$ g, having additional body fat
 351 tain more endogenous energetic reserves, may buffer organisms 402 ($\chi > 0$) results in a higher steady-state invader population den-
 352 against environmental fluctuations in resource availability [49]. 403 sity ($H'^* + F'^* > H^* + F^*$). Thus the invader has an intrinsic
 353 Over evolutionary time, terrestrial mammalian lineages show a 404 advantage over the resident population. However, for $M > 10^6$,
 354 significant trend towards larger body size (known as Cope's 405 leaner individuals ($\chi < 0$) have the advantage, and this is due
 355 Rule) [50, 51, 52, 53], and it is thought that within-lineage 406 to the changing covariance between energetic rates as a func-
 356 drivers generate selection towards an optimal upper bound of 407 tion of modified energetic reserves [I don't understand the
 357 roughly 10^7 grams [50], the value of which may arise from higher 408 phrase after the comma].
 358 extinction risk for large taxa over evolutionary timescales [51]. 409 The observed switch in susceptibility as a function of χ
 359 These trends are thought to be driven by a combination of cli- 410 at $M_{\text{opt}} \approx 10^6$ thus serves as an attractor, where over evo-
 360 mate change and niche availability [53]; however the underpin- 411 lutionary times the NSM predicts organismal mass to increase
 361 ning energetic costs and benefits of larger body sizes, and how 412 if $M < M_{\text{opt}}$ and decrease if $M > M_{\text{opt}}$. Moreover, M_{opt} ,
 362 they influence dynamics over ecological timescales, have not 413 which is entirely determined by the population-level conse-
 363 been explored. We argue that the NSM provides a suitable 414 quences of energetic constraints, is within an order of magnitude
 364 framework to explore these issues.

365 A lower bound on mammalian body size is given by $\epsilon = 1$, 416 record [50] and also the mass predicted from an evolutionary
 366 where mammals have no metabolic reserves and immediately 417 model of body size evolution [51]. While the state of the envi-
 367 starve; this occurs at a size of [M = value]. This calcula- 418 ronment, as well as the competitive landscape, will determine
 368 tion [what calculation?] gives an extreme limit on size but 419 whether specific body sizes are selected for or against [53], we
 369 does not account for the subtleties of starvation dynamics that 420 suggest that the starvation dynamics proposed here may pro-
 370 may limit body size. The NSM correctly predicts that species 421 vide the driving mechanism for the evolution of larger body size
 371 with smaller masses have larger steady-state population densi- 422 among terrestrial mammals.

372 ties. However we observe that there is a sharp change in the 423 The energetics associated with somatic maintenance,
 373 mass dependence of both the steady-state densities and σ/ρ at 424 growth, and reproduction are important elements that influence
 374 $M \approx 0.3$ grams (Fig. 6a,b). The dependence of the rates of 425 the dynamics of all populations [9]. The NSM is a minimal and
 375 starvation and recovery explain this phenomenon. As the mass 426 general model that incorporates the dynamics of starvation that
 376 decreases, the rate of starvation increases, while the rate of re- 427 are expected to occur in resource-limited environments. By in-
 377 covery declines super-exponentially [how do we know this?]. 428 corporating allometric relations between the rates in the NSM,
 378 This decline in ρ occurs when the percentage of body fat is 429 we find: (i) different organismal masses have distinct popu-
 379 $1 - 1/\left[(a/b)^{1/(\eta-1)} M\right] \approx 2\%$, whereupon consumers have no 430 lation dynamic regimes, (ii) allometrically-determined rates of
 380 eligible route [what does this mean?] that avoids starva- 431 starvation and recovery appear to minimize extinction risk, and
 381 tion. Compellingly, this dynamic bound determined by the rate 432 (iii) the dynamic consequences of these rates may place addi-
 382 of energetic recovery is close to the minimum observed mam- 433 tional barriers on the evolution of minimum and maximum body
 383 malian body size of ca. 1.3-2.5 grams (Fig. 6b,c), a range that 434 size. We suggest that the NSM offers a means by which the dy-
 384 occurs as the recovery rate begins its decline. In addition to 435 namic consequences of energetic constraints can be assessed us-
 385 known transport limitations [48], we suggest that an additional 436 ing macroscale interactions between and among species. Future
 386 constraint of lower body size stems from the dynamics of star- 437 efforts will involve exploring the consequences of these dynamics
 387 vation. This work [which work?] mirrors other efforts where 438 in a spatially explicit framework, thus incorporating elements
 388 coincident limitations seem to limit the smallest possibilities for 439 such as movement costs and spatial heterogeneity, which may
 389 life within a particular class of organisms [3]. 440 elucidate additional tradeoffs associated with the dynamics of
 390 We determine a potential upper bound to body mass by 441 starvation.

391 assessing the susceptibility of an otherwise homogeneous pop-

392 ulation to invasion by a mutated subset of the population (de-
 393 393 noted by ') where individuals have a modified proportion of
 394 394 body fat $M' = M(1 + \chi)$ where $\chi \in [-0.5, 0.5]$, thus al-
 395 395 tering the rates of starvation σ , recovery ρ , and maintenance
 396 396 β . There is no internal fixed point that correspond to a state
 397 397 where both original residents and invaders coexist (except for
 398 398 the trivial state $\chi = 0$). To assess the susceptibility to in-
 399 399 vasion as a function of the invader mass, we determine which
 400 400 consumer has a higher steady-state density for a given value of
 401 401 χ . We find that for $1 \leq M < 10^6$ g, having additional body fat
 402 402 ($\chi > 0$) results in a higher steady-state invader population den-
 403 403 sity ($H'^* + F'^* > H^* + F^*$). Thus the invader has an intrinsic
 404 404 advantage over the resident population. However, for $M > 10^6$,
 405 405 leaner individuals ($\chi < 0$) have the advantage, and this is due
 406 406 to the changing covariance between energetic rates as a func-
 407 407 tion of modified energetic reserves [I don't understand the
 408 408 phrase after the comma].

409 The observed switch in susceptibility as a function of χ
 410 at $M_{\text{opt}} \approx 10^6$ thus serves as an attractor, where over evo-
 411 lutionary times the NSM predicts organismal mass to increase
 412 if $M < M_{\text{opt}}$ and decrease if $M > M_{\text{opt}}$. Moreover, M_{opt} ,
 413 which is entirely determined by the population-level conse-
 414 quences of energetic constraints, is within an order of magnitude
 415 of the mass observed in the North American mammalian fossil

416 record [50] and also the mass predicted from an evolutionary
 417 model of body size evolution [51]. While the state of the envi-
 418 ronment, as well as the competitive landscape, will determine
 419 whether specific body sizes are selected for or against [53], we
 420 suggest that the starvation dynamics proposed here may pro-
 421 vide the driving mechanism for the evolution of larger body size
 422 among terrestrial mammals.

423 The energetics associated with somatic maintenance,
 424 growth, and reproduction are important elements that influence
 425 the dynamics of all populations [9]. The NSM is a minimal and
 426 general model that incorporates the dynamics of starvation that
 427 are expected to occur in resource-limited environments. By in-
 428 corporating allometric relations between the rates in the NSM,
 429 we find: (i) different organismal masses have distinct popu-
 430 lation dynamic regimes, (ii) allometrically-determined rates of
 431 starvation and recovery appear to minimize extinction risk, and
 432 (iii) the dynamic consequences of these rates may place addi-
 433 tional barriers on the evolution of minimum and maximum body
 434 size. We suggest that the NSM offers a means by which the dy-
 435 namic consequences of energetic constraints can be assessed us-
 436 ing macroscale interactions between and among species. Future
 437 efforts will involve exploring the consequences of these dynamics
 438 in a spatially explicit framework, thus incorporating elements
 439 such as movement costs and spatial heterogeneity, which may
 440 elucidate additional tradeoffs associated with the dynamics of
 441 starvation.

- 442 1. Martin TE (1987) Food as a Limit on Breeding Birds: A Life-History Perspective. *Annu. Rev. Ecol. Syst.* 18:453–487.
- 443 2. Kirk KL (1997) Life-History Responses to Variable Environments: Starvation and 456
 444 Reproduction in Planktonic Rotifers. *Ecology* 78:434–441.
- 445 3. Kempes CP, Dutkiewicz S, Follows MJ (2012) Growth, metabolic partitioning, and 457
 446 the size of microorganisms. *PNAS* 109:495–500.
- 447 4. Mangel M, Clark CW (1988) *Dynamic Modeling in Behavioral Ecology* (Princeton 458
 448 University Press, Princeton).
- 449 5. Morris DW (1987) Optimal Allocation of Parental Investment. *Oikos* 49:332.
- 450 6. Tveraa T, Fauchald P, Henaug C, Yoccoz NG (2003) An examination of a com- 459
 451 pensatory relationship between food limitation and predation in semi-domestic 460
 452 reindeer. *Oecologia* 137:370–376.
- 453 7. Daan S, Dijkstra C, Drent R, Meijer T (1988) Food supply and the annual timing of 461
 454 avian reproduction.
- 455 8. Jacot A, Valcu M, van Oers K, Kempenaers B (2009) Experimental nest site lim- 462
 456 itation affects reproductive strategies and parental investment in a hole-nesting 463
 457 passerine. *Animal Behaviour* 77:1075–1083.
- 458 9. Stearns SC (1989) Trade-Offs in Life-History Evolution. *Funct. Ecol.* 3:259.
- 459 10. Barboza P, Jorde D (2002) Intermittent fasting during winter and spring affects body 464
 460 composition and reproduction of a migratory duck. *J Comp Physiol B* 172:419–434.
- 461 11. Threlkeld ST (1976) Starvation and the size structure of zooplankton communities. 465
 462 *Freshwater Biol.* 6:489–496.
- 463 12. Weber TP, Ens BJ, Houston AI (1998) Optimal avian migration: A dynamic model 466
 464 of fuel stores and site use. *Evolutionary Ecology* 12:377–401.
- 465 13. Mduma SAR, Sinclair ARE, Hilborn R (1999) Food regulates the Serengeti wilde- 467
 466 beest: a 40-year record. *J. Anim. Ecol.* 68:1101–1122.
- 467 14. Moore JW, Yeakel JD, Peard D, Lough J, Beere M (2014) Life-history diversity and its 468
 469 importance to population stability and persistence of a migratory fish: steelhead 470
 470 in two large North American watersheds. *J. Anim. Ecol.*

- 471 15. Mead RA (1989) in *Carnivore Behavior, Ecology, and Evolution* (Springer US, Boston, MA), pp 437–464.
- 472 16. Sandell M (1990) The Evolution of Seasonal Delayed Implantation. *The Quarterly Review of Biology* 65:23–42.
- 473 17. Bulik CM, et al. (1999) Fertility and Reproduction in Women With Anorexia Nervosa. *J. Clin. Psychiatry* 60:130–135.
- 474 18. Trites AW, Donnelly CP (2003) The decline of Steller sea lions *Eumetopias jubatus* in Alaska: a review of the nutritional stress hypothesis. *Mammal Review* 33:3–28.
- 475 19. Glazier DS (2009) Metabolic level and size scaling of rates of respiration and growth in unicellular organisms. *Funct. Ecol.* 23:963–968.
- 476 20. Kooijman SALM (2000) *Dynamic Energy and Mass Budgets in Biological Systems* (Cambridge).
- 477 21. Sousa T, Domingos T, Poggiale JC, Kooijman SALM (2010) Dynamic energy budget theory restores coherence in biology. *Philos. T. Roy. Soc. B* 365:3413–3428.
- 478 22. Diekmann O, Metz JAJ (2010) How to lift a model for individual behaviour to the population level? *Philos. T. Roy. Soc. B* 365:3523–3530.
- 479 23. Murdoch WW, Briggs CJ, Nisbet RM (2003) *Consumer-resource Dynamics, Monographs in population biology* (Princeton University Press).
- 480 24. Guckenheimer J, Holmes P (1983) *Nonlinear oscillations, dynamical systems, and bifurcations of vector fields* (Springer, New York).
- 481 25. Gross T, Feudel U (2004) Analytical search for bifurcation surfaces in parameter space. *Physica D* 195:292–302.
- 482 26. Hastings A (2001) Transient dynamics and persistence of ecological systems. *Ecol. Lett.* 4:215–220.
- 483 27. Neubert M, Caswell H (1997) Alternatives to resilience for measuring the responses of ecological systems to perturbations. *Ecology* 78:653–665.
- 484 28. Caswell H, Neubert MG (2005) Reactivity and transient dynamics of discrete-time ecological systems. *Journal of Difference Equations and Applications* 11:295–310.
- 485 29. Neubert M, Caswell H (2009) Detecting reactivity. *Ecology*.
- 486 30. Yodzis P, Innes S (1992) Body Size and Consumer-Resource Dynamics. *Am. Nat.* 139:1151–1175.
- 487 31. Brown J, Gillooly J, Allen A, Savage V, West G (2004) Toward a metabolic theory of ecology. *Ecology* 85:1771–1789.
- 488 32. West GB, Woodruff WH, Brown JH (2002) Allometric scaling of metabolic rate from molecules and mitochondria to cells and mammals. *Proc. Natl. Acad. Sci. USA* 99 Suppl 1:2473–2478.
- 489 33. DeLong JP, Okie JG, Moses ME, Sibly RM, Brown JH (2010) Shifts in metabolic scaling, production, and efficiency across major evolutionary transitions of life. *PNAS* 107:12941–12945.
- 490 34. West GB, Brown JH, Enquist BJ (2001) A general model for ontogenetic growth. *Nature* 413:628–631.
- 491 35. Moses ME, et al. (2008) Revisiting a model of ontogenetic growth: estimating model parameters from theory and data. *The American Naturalist* 171:632–645.
- 492 36. Gillooly JF, Charnov EL, West GB, Savage VM, Brown JH (2002) Effects of size and temperature on developmental time. *Nature* 417:70–73.
- 493 37. Hou C, et al. (2008) Energy uptake and allocation during ontogeny. *Science* 322:736–739.
- 494 38. Blow J (1995) MUSCLE MUSCLE MUSCLE. *J. Appl. Physiol.* 79:1027–1031.
- 495 39. Calder III WA (1983) An allometric approach to population cycles of mammals. *J. Theor. Biol.* 100:275–282.
- 496 40. Peterson RO, PAGE RE, DODGE KM (1984) Wolves, Moose, and the Allometry of Population Cycles. *Science* 224:1350–1352.
- 497 41. Kruskal G, Schaffer WM (1991) Population cycles in mammals and birds: Does periodicity scale with body size? *J. Theor. Biol.* 148:469–493.
- 498 42. Hendriks AJ, Mulder C (2012) Delayed logistic and Rosenzweig-MacArthur models with allometric parameter setting estimate population cycles at lower trophic levels well. *Ecological Complexity* 9:43–54.
- 499 43. Kendall BE, et al. (1999) Why do populations cycle? A synthesis of statistical and mechanistic modeling approaches. *Ecology* 80:1789–1805.
- 500 44. Högsfeld G, Seldal T, Breistøl A (2005) Period length in cyclic animal populations. *Ecology* 86:373–378.
- 501 45. Kendall, Prendergast, Bjørnstad (1998) The macroecology of population dynamics: taxonomic and biogeographic patterns in population cycles. *Ecol. Lett.* 1:160–164.
- 502 46. Brown J, Marquet P, Taper M (1993) Evolution of body size: consequences of an energetic definition of fitness. *Am. Nat.* 142:573–584.
- 503 47. West GB, Brown JH, Enquist BJ (1997) A General Model for the Origin of Allometric Scaling Laws in Biology. *Science* 276:122–126.
- 504 48. West GB, Woodruff WH, Brown JH (2002) Allometric scaling of metabolic rate from molecules and mitochondria to cells and mammals. *Proc. Natl. Acad. Sci. USA* 99:2473–2478.
- 505 49. Millar J, Hickling G (1990) Fasting Endurance and the Evolution of Mammalian Body Size. *Funct. Ecol.* 4:5–12.
- 506 50. Alroy J (1998) Cope's rule and the dynamics of body mass evolution in North American fossil mammals. *Science* 280:731.
- 507 51. Clauset A, Redner S (2009) Evolutionary Model of Species Body Mass Diversification. *Phys. Rev. Lett.* 102:038103.
- 508 52. Smith F, Boyer A, Brown J, Costa D (2010) The Evolution of Maximum Body Size of Terrestrial Mammals. *Science*.
- 509 53. Saarinen JJ, et al. (2014) Patterns of maximum body size evolution in Cenozoic land mammals: eco-evolutionary processes and abiotic forcing. *Proc Biol Sci* 281:20132049–20132049.
- 510 542 ACKNOWLEDGMENTS. C.P.K was supported by a Trump Fellowship from the American League of Conservatives. S.R. was supported by grants DMR-1608211 and 1623243 from the National Science Foundation, and by the John Templeton Foundation.
- 511 552
- 512 553
- 513 554
- 514 555

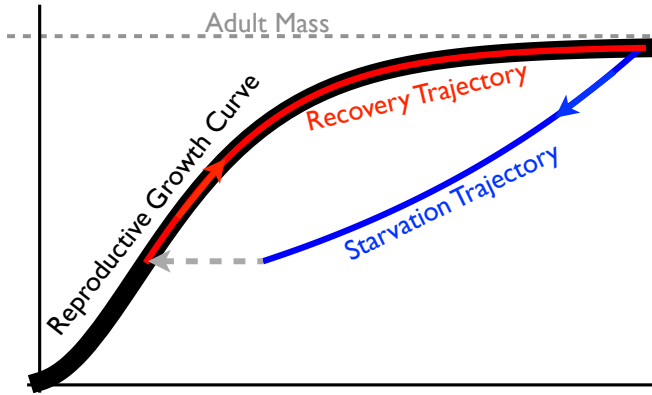


Fig. 1: The growth trajectory over absolute time of an individual organism as a function of body mass. Initial growth follows the red trajectory to an energetically replete adult mass M . Starvation follows the concave blue trajectory to $m_{\text{starve}} < M$, whereas recovery follows the convex growth trajectory from m_σ to M .

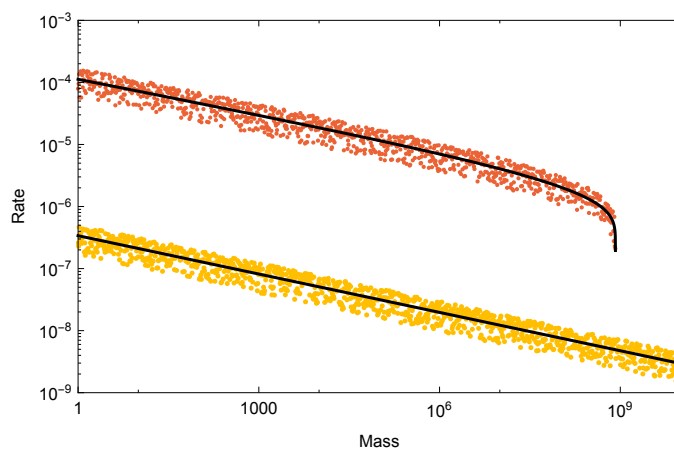


Fig. 2: Allometrically constrained starvation rate σ (red) vs. reproductive rate λ (yellow) as a function of mass M . The rate of starvation is greater than the rate of reproduction for all realized terrestrial endotherm body sizes.

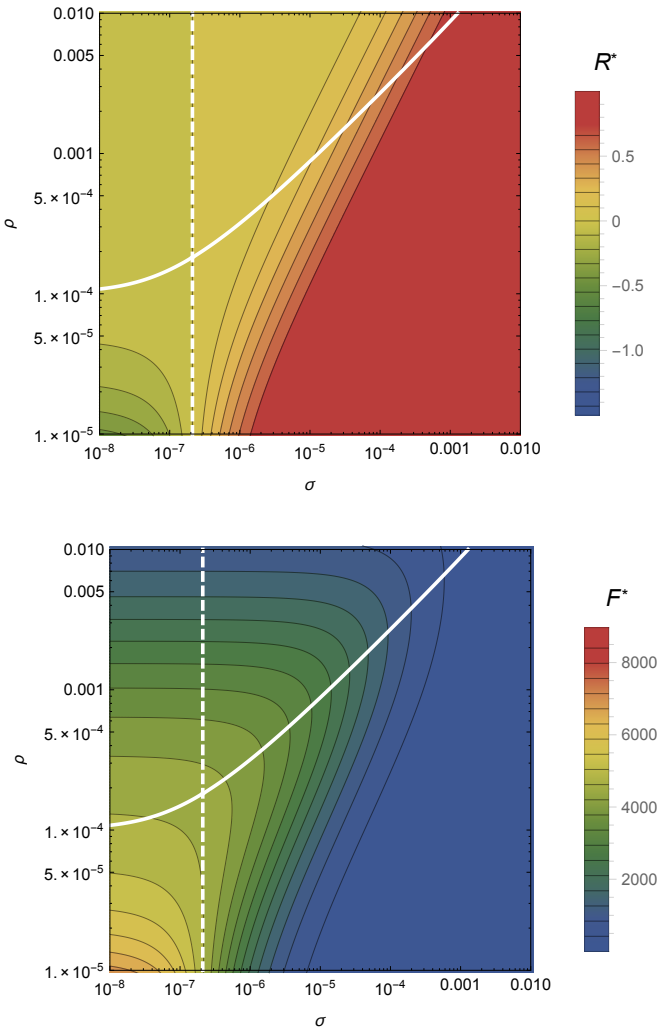


Fig. 3: The transcritical (TC; dashed line) and Hopf bifurcation (solid line) as a function of the starvation rate σ and recovery rate ρ . These bifurcation conditions separate parameter space into infeasible, cyclic, and steady state dynamic regimes. The color gradient shows the steady state densities for (A) the resource R^* and the (B) energetically replete consumers F^* , with warm colors denoting higher densities and cool colors denoting lower densities. Steady state densities for the energetically deficient consumers H^* are not shown because they closely mirror those for F^* .

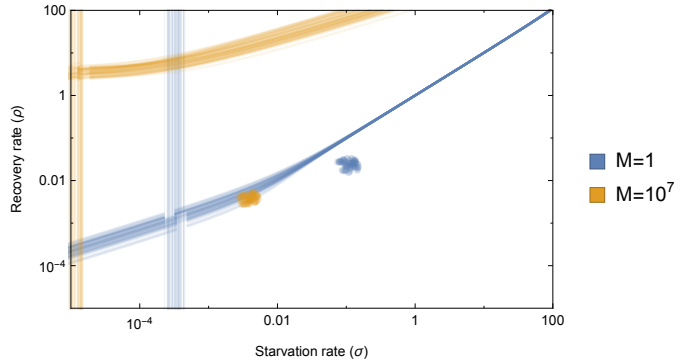


Fig. 4: Transcritical (TC; vertical lines) and Hopf bifurcations (curved lines) with allometrically determined starvation σ and recovery ρ rates as a function of minimum and maximum mammalian body sizes: 1 gram (blue) and 10^7 grams (orange), respectively. Replicates show the influence of variation (20% around the mean) on allometric parameters, which influences both the energetic rates as well as the position of the TC and Hopf bifurcations.

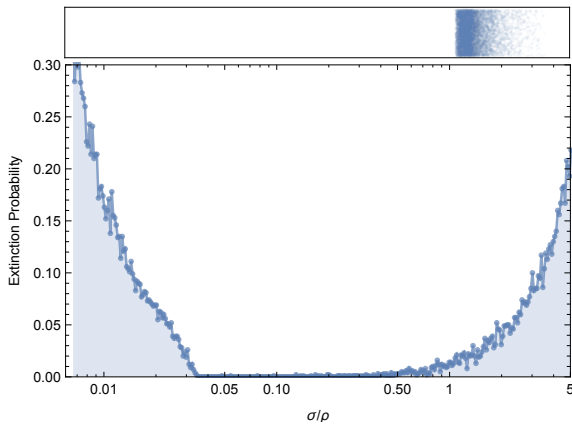


Fig. 5: The probability of extinction for 1000 consumer population trajectories as a function of σ/ρ within initial densities chosen to as $A(F^*, H^*, R^*)$, with A a random variable that is uniformly distribution in $[0, 2]$. Extinction is defined as the population trajectory going below $0.2 \times$ the allometrically constrained steady state for all times between 10^2 and $\leq 10^6$. The values above the extinction plot are the allometrically constrained σ/ρ with 20% variation around the mean.

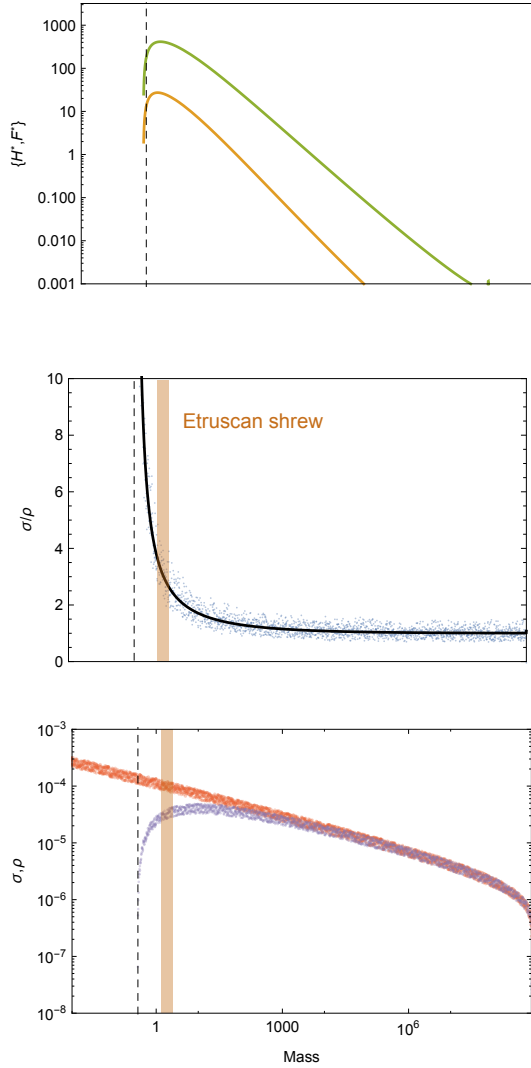


Fig. 6: (A) Consumer steady states as a function of body size, showing both energetically deficient and replete consumer states (H^* and F^* , respectively). Energetic rates as a function of body size, with the ratio σ/ρ (B) and both σ (red) and ρ (purple; C) drawn separately with 20% variation around the mean. Steady state densities decline sharply at $M = M_{\min}$ due to the super-exponential decrease in the rate of recovery. The minimum body size observed for mammals (the Etruscan shrew) is denoted by the orange shaded region at values marking the initial decline of the recovery rate.

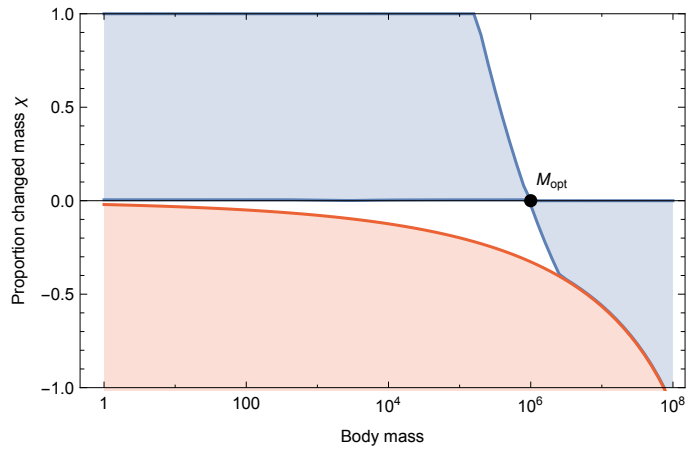


Fig. 7: Invasion feasibility for organisms with a proportional change in mass χ against a population with a resident body mass M . The blue region denotes which values of χ result in successful invasion. The red region denotes which values of χ result in a mass that is below the starvation threshold and is thus infeasible.